

# Capture Efficiency of the Aaberg Exhaust Hood and its Variation with Spatial Arrangement

Vladimir Krejci, Miroslav Jicha, Milan Pavelek  
krejci.v@fme.vutbr.cz

Brno University of Technology, Faculty of Mechanical Engineering  
Department of Thermodynamics and Environmental Engineering  
Brno Czech Republic

phone: +420 541 143 284 fax: +420 541 143 365 <http://ottp.fme.vutbr.cz>

## Abstract

*The paper deals with CFD simulations of a reinforced exhaust system (the Aaberg exhaust hood in particular). The reinforced suction effect is achieved by means of radial jet release. The radial jet deforms the flow pattern in front of the hood to a directional flow pattern. Unfortunately, the presence of an obstacle, such as a welding bench, leads to a defective operation of the hood. A number of CFD simulations has been undertaken in order to assess the effect of the obstacle size, its distance to the hood, and the hood declination from the normal of the obstacle surface, on the flow pattern and consequently the capture efficiency of the hood. Capture efficiency of selected cases was evaluated. For the purpose of capture efficiency evaluation, a heat source was defined within the model that imitated a metal arc welding process and introduced similar heat input into the domain altogether with a release of a passive scalar. The scalar concentration was then evaluated at the hood opening, thus capture efficiency could be calculated. The results of simulations indicate that the hood operation depends on the spatial arrangement of the hood and the obstacle. The best performance was achieved when the hood axis was aligned with the obstacle surface normal or the misalignment was small. Greater misalignment can be tolerated when the obstacle size is smaller than the hood-to-obstacle distance only.*

## Introduction

The requirement of improved working environment leads to an effort being aimed at better design of ventilation systems that control the inner environment of a workplace. Although diseases of respiratory system are on decrease in the Czech Republic, the part of people who suffer from this kind of diseases is large; the third highest among the vocational diseases in the Czech Republic (Institute of Health Information and Statistics of the Czech Republic) [1], [2] and similarly in Switzerland (SUVA) [3]. As people spend considerable part of their lives at work, great attention is paid to protect them from being harmed by the industrial process they take part in. Additionally, there are technological processes where close control of the working environment is crucial for them to be feasible. These issues led the authors to carry out investigation of a particular local ventilation system called the Aaberg exhaust hood and its operation by means of numerical methods.

A ventilation system is employed to control pollutant level of indoor environment of a building. The ventilation system can achieve its task in many ways and, according to air change rate within the ventilated space, the system can be either a global or a local one. The global ventilation system controls pollution level over the whole ventilated space providing it with fresh air and diluting the pollution concentration to such a value it cannot do any harm to the occupants of the space. On the contrary, the local ventilation system provides high comfort to a close area of the terminal device thus where needed only. It can meet the required air quality by delivering fresh air to the breathing zone of an occupant (personal ventilation) or extract polluted air at location of its release (local exhaust ventilation systems).

Among the local exhaust ventilation systems, the exhaust hoods are quite common. An exhaust hood controls the pollution level within a space by capturing pollution as close to its source as possible. Due to its principle (local control of the pollution), the local ventilation system compares favourably to the global systems as when looking at energy demands, especially when there is a strong source of pollution that is concentrated to a small area so it can be easily located. On the other hand the systems of local extraction suffer from not being too efficient when the pollution source moves away from them. This means, the hood location is very important and the distance between the contaminant source and the hood should be as small as possible in order to achieve good performance. If

an insensible hood location is chosen then the hood may also interfere with the worker hence limit its operational area.

### The Aaberg Hood Principle

The traditional exhaust hood employed to extract polluted air from a workplace makes use of air extraction only (see Figure 1). Its performance can be varied by means of increasing of the extracted air flow rate, or via adaptations to the terminal device – hood – which is mounted at the end of the extraction duct and affects the flow pattern across the space of consideration. One of the common adaptations that enhance the suction effect a flange fit to the hood. The flange partially blocks the flow paths coming from behind of the hood thus increased suction is achieved. The flange also affects the hood entry pressure loss in a positive way, leading to less power need to run fans of the exhaust system.

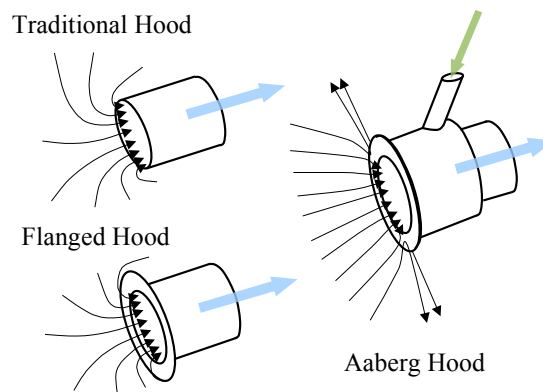


Figure 1 Types of exterior exhaust hoods

C.P. Aaberg, a Danish engineer, proposed to combine extraction of the polluted air and air supply for a pig stable ventilation [4]. The air supply forms a jet which blows in the perpendicular direction to the direction of air extraction. The supplied air creates a virtual flange of much greater extension, when compared with the flanged hood. The virtual flange amplifies the extraction in the same way it does it with the traditional flanged hood. Furthermore, the jet entrains surrounding fluid, generating additional force for improved suction of the hood. In this way, a directional flow pattern is formed in front of the hood.

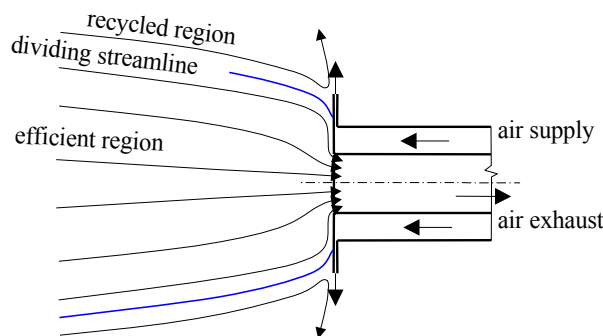


Figure 2 The Aaberg hood - flow pattern and regions

Figure 2 shows flow regions encountered with the Aaberg hood as suggested by Høgsted [5]. The regions follow an assumption that pollution cannot travel across the area in front of the hood (no cross flow and low turbulence and diffusion).

Hylgård [6] has established a hood operational parameter as a ratio of supply to extracted momentum fluxes, see equation (1). The higher the ratio, the narrower the efficient region and higher capture efficiency.

$$I = \frac{\dot{m}_{jet} u_{jet}}{\dot{m}_{ext} u_{ext}}. \quad (1)$$

The capture efficiency of a hood is assessed, knowing the released and captured mass fluxes of pollution, according to the following formula:

$$\eta_{captured} = \frac{\dot{m}_{captured}}{\dot{m}_{released}} \times 100 \%. \quad (2)$$

## Description of the models

For the purpose of this study two geometries were considered; a box-like geometry ( $W \times L \times H = 4 \times 4 \times 3$  m) and a sector (6 m in diameter, 6 m in length and  $4^\circ$  of central angle of the sector). In the central location (to the box), an exhaust hood was located over a workbench according to the scheme depicted in Figure 3. Three bench-hood (BD) distances and bench sizes (BS) were considered in simulations. The distances and sizes were derived from the hood opening diameter,  $d$ , as its integer multiples (3, 5, 7 and 5, 10, 15, respectively). In order to distinguish the simulations, a code was formed so the version 'a30\_d3\_b15\_3D' means: the angle of hood declination  $30^\circ$ , the bench-hood distance  $3d$ , the workbench size  $15d$ , three dimensional case. The hood opening diameter,  $d$ , was kept fixed throughout all of the simulations and was equal to 0.08 m. Other geometrical parameters of the hood were: flange diameter,  $D$ , of 0.2 m, and supply slot width,  $b$ , of 0.004 m.

Imposed boundary conditions were: prescribed pressure at ceiling of the computational domain to balance the extraction and supply flow rates. The extracted and supplied flow rates ( $120 \text{ m}^3/\text{h}$  and  $65.6 \text{ m}^3/\text{h}$ , respectively) were set up via velocity inlet (uniform velocity profile). These parameters led to momentum fluxes ratio of 0.6 which is an optimum value for the best performance under crossflow conditions according to Pedersen [7].

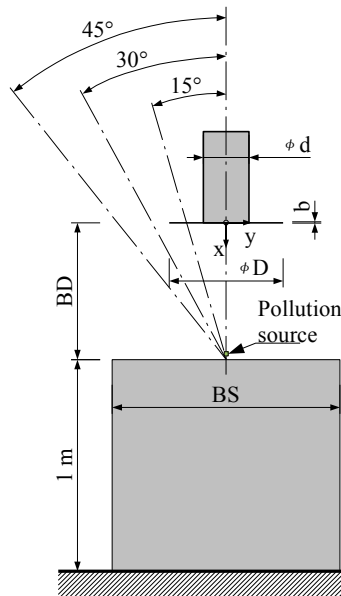


Figure 3 Schematic view of the solved system

The 2D (sector) and 3D (box) geometry meshes consisted of about 12 000 and 700 000 hexahedral cells, respectively. Second order MUSCL type spatial discretization scheme with TVD limiters was employed [8] for the simulations. The workbench was treated in two ways for 2D simulations: a solid block bench (Figure 3) and a baffle (imitating just the workbench board). A solid block bench was used in 3D simulations. It should be also mentioned here, the workbench shape (cross section) differed for 2D and 3D simulations. Due to the axisymmetric 2D domain, the bench inherited a circular

cross section. On the other hand, the 3D bench was considered to be more alike a real one thus a block shape of a square cross section was employed.

As the simulations showed unsteady behaviour in some cases, it was decided to run them in transient mode for 30 second restarting the simulations from pre-solved steady state results. The results were then averaged over the whole time period. For the time discretization, Crank-Nicolson scheme was employed. Turbulent flow was modelled with the use of  $k-\varepsilon$  turbulence model as it was found the best for the radial jet modelling [9], [10].

3D simulations only were solved for pollution and heat release thus the only ones giving capture efficiencies. The pollution source was modelled in two ways. The first way was release of massless particles by the source There were 100 of particles released in the centre of the bench throughout an area of 0.04 by 0.04 m and 0.02 m over the bench surface. The particles did not interact with the fluid except that they were entrained by it. The capture efficiency was then evaluated by counting the particles that left the computational domain via the exhaust opening. Another way employed to evaluate the capture efficiency was release of a passive scalar into a computational domain at location 0.01 m over the bench surface; the passive scalar being an ideal tracer and its mass flow rate 1 mg/s. Additionally to the scalar, heat was produced by the source at rate of 40 W [11]. Both pollution and heat were released within a cube of 0.02 m edge length. The first approach applied to isothermal solution, the later to the solution in which heat was released along with the passive scalar thus non-isothermal solution.

## Results and their discussion

### Isothermal solution

Results of 2D and 3D simulations are compared in Figure 4. It is clear the simplified sector geometry can be used for most of the simulations where there will be no cause of asymmetry (hood diverted from the workbench normal). When the hood was as close as  $3 \times d$  in distance from the bench, the actual bench shape began influencing the flow (circular in 2D and square shaped in 3D). The vicinity of the bench increased the Coanda effect and the irregular bench shape (square) in 3D caused the jet to attach and detach from the bench surface. The 30 seconds time averaging then resulted in increased velocity magnitude near the bench surface.

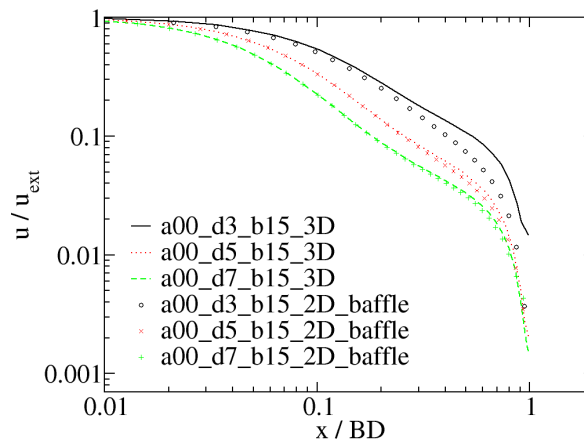


Figure 4 Comparison of velocity magnitude decays for 2D and 3D simulations

The effect of bench presence on a flow patten in front of the hood is depicted in Figure 5. When there was no obstacle to the flow (no bench), the velocity decay tended to be linear in logarithmically scaled coordinates. This did not apply to the flow with an obstacle. The velocity decay was more dramatical because the obstacle acted as blockage to the flow which had to be passed by.

Figure 6 shows velocity decays as functions of bench size and distance. The decay was almost not affected when the hood operated in traditional mode (no jet) no matter what the actual bench size was.

Similar influence was encountered with the hood operating in Aaberg mode but the decay is remarkably more gradual in comparison with the traditional hood. Locating the hood closer ( $3 \times d$ ) to the bench of a small size ( $5 \times d$ ) made the decay even more moderate so high air speed alike to the one at the supply slot prevailed significant part of the domain between the hood and the obstacle; on the other hand, the effect of obstacle magnified as well.

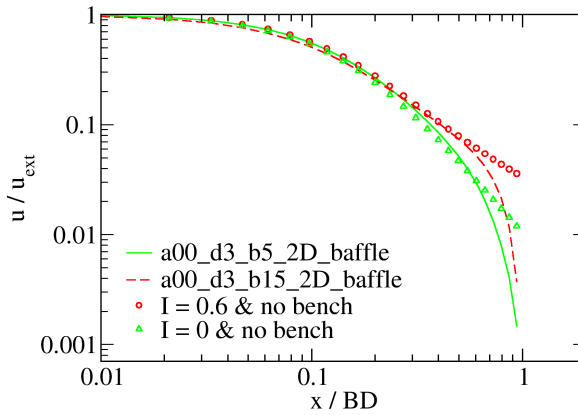


Figure 5 Effect of the bench presence and size

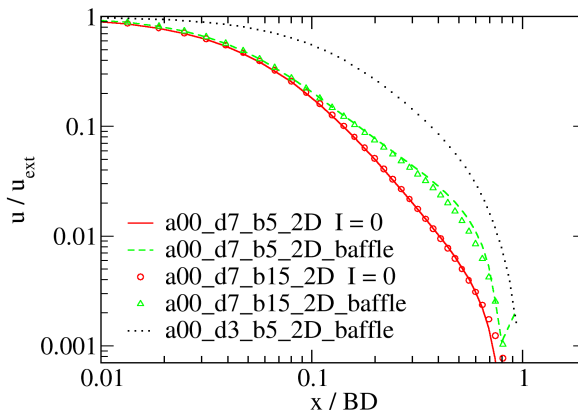


Figure 6 Effects of the bench distance and size

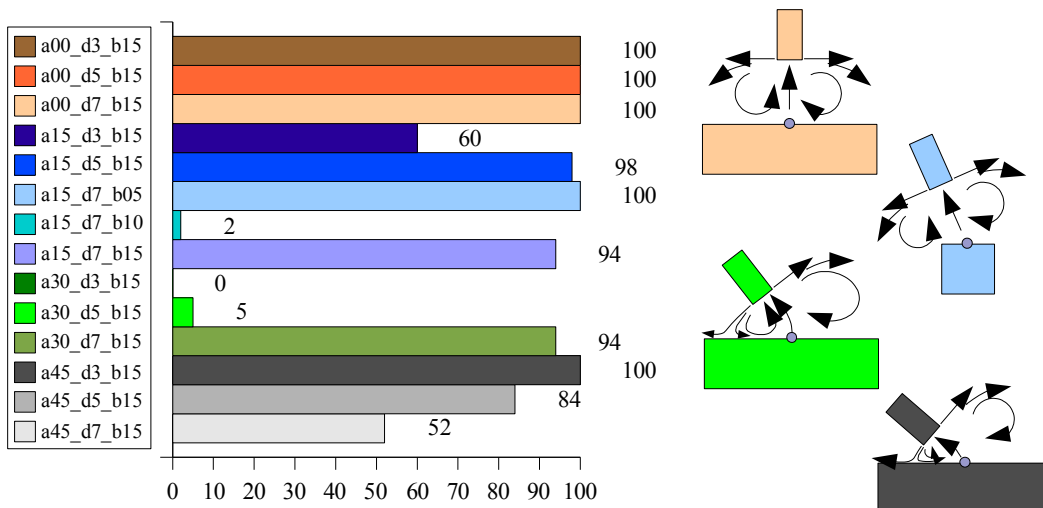


Figure 7 Capture efficiency in % and corresponding flow patterns

Figure 7 shows there is a relationship between capture efficiency of the Aaberg hood and its spatial arrangement to the bench. The hood performance is good when the hood is located above the bench

centre as the jet is aligned with the bench surface, thus not too affected by it. If the hood was orientated in such a manner the declination angle was  $15^\circ$ , the jet become unstable, especially with the bench of a large size. The larger the distance the more stable the jet was but it was not so if the bench was correspondingly resized. There was an exception in the trend of which flow pattern is illustrated in Figure 8. There on can see the reason for such a bad performance of the hood (capture efficiency about 2 %). The flow pattern was so deformed all the particles generated at the bench centre were blown away along the bench surface.

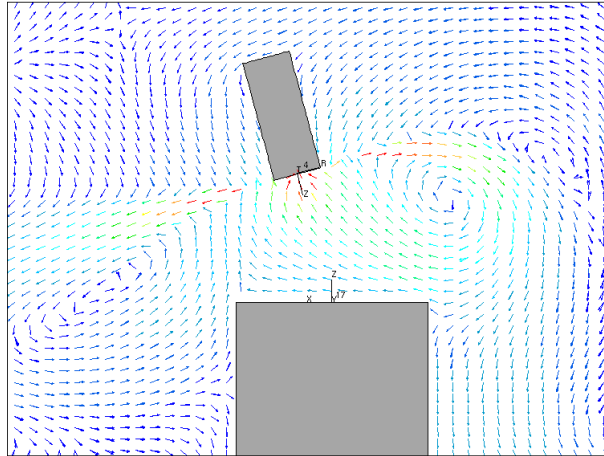


Figure 8 Flow pattern for the case when the hood declination angle was  $15^\circ$ , the bench size  $10 \times d$  and bench to hood distance  $7 \times d$

It was this what deteriorated the performance of the Aaberg hood. The jet made it impossible for the hood to catch almost any particles at declination angle of  $30^\circ$  when the distance to the workbench was small. The presence of the bench caused the misaligned jet to attach to it so a short circuit happened to a part of the jet. The short circuit flow was able to blow away the particles depending on location of attachment curve on the bench surface.

### Temperature dependent solution

Figure 9 represents the changes in flow patterns and the corresponding pollution concentration in ppm in front of the hood. The colours the hoods are assigned correspond to the case as labeled in the Figure 10. The code used to distinguish version in this part of the study was adapted so 'a00\_120ext' means the hood declination angle was  $0^\circ$  and  $120 \text{ m}^3/\text{h}$  of air was extracted by the hood. The Aaberg principle operating hood was operating at the basic extracted flow rate of  $120 \text{ m}^3/\text{h}$ .

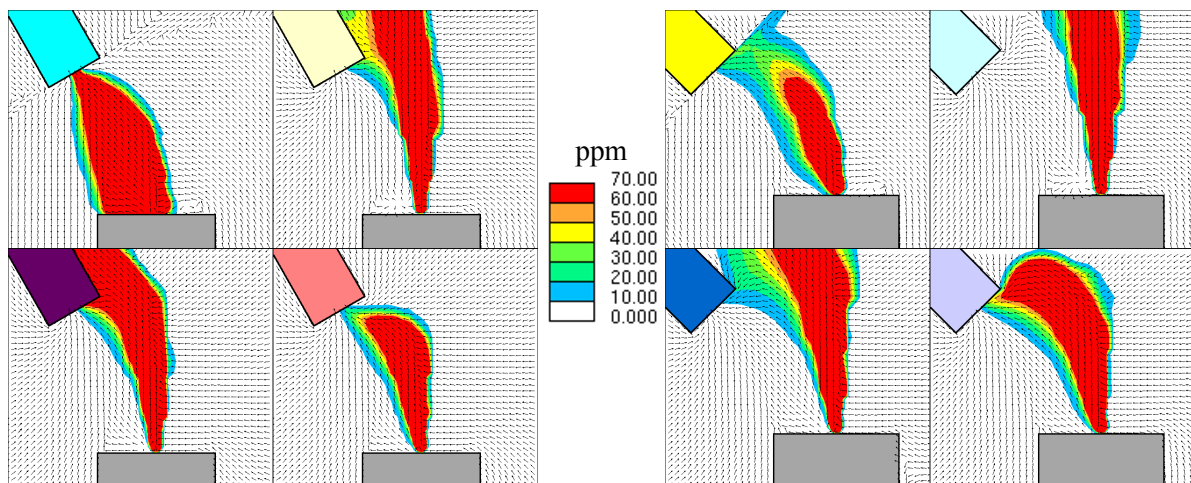


Figure 9 Flow pattern and hood performance comparison at hood declination angle of  $30^\circ$  (left) and  $45^\circ$  (right); upper left picture of the set stands for the Aaberg hood operating at  $I = 0.6$

All the figures were obtained by time averaging of the results over the last 30 seconds of simulations. The figures compare an Aaberg hood (upper-left one) with a traditional flanged hood (the remaining three). The traditional hood depicted operates at flow rates 120 m<sup>3</sup>/h (base), and doubled and quadrupled flow rates of extracted air. It is clear that the hot plume creates quite strong air movement that can be overcome by high flow rates only. The hood performance worsened seriously with increased declination angle of the hood, nonetheless this feature was less significant with the Aaberg hood. The traditional flanged hood was able to capture pollution if it was located just above its source. But when diverted from this location, the flow rate had to be doubled or eventually quadrupled to collect all the pollution. The Aaberg hood lack of efficiency at low angle of declination was caused by the radial jet and the plume instability as the efficient region is quite narrow and the unstable plume can cross the dividing line. When the plume was caught by a side located hood, its instability was partially suppressed so higher efficiency was achieved.

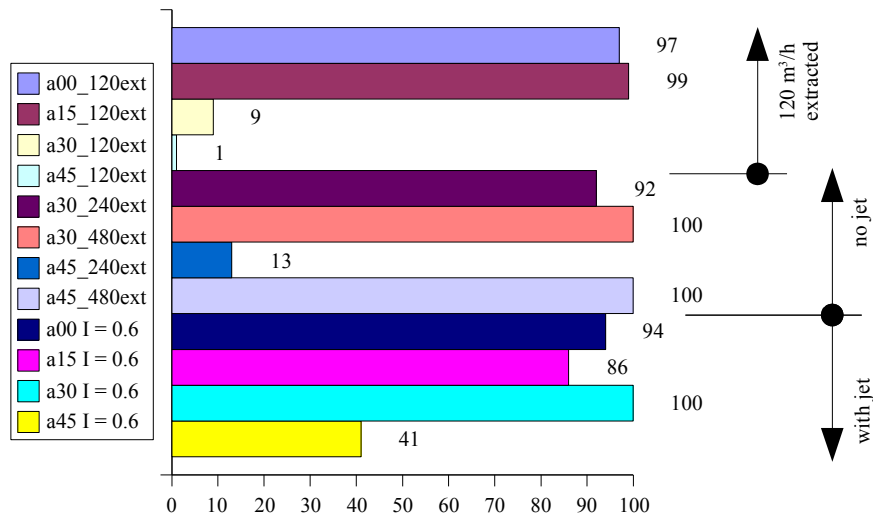


Figure 10 Capture efficiencies in % as a function of the hood declination

## Conclusions

The presented article has revealed the effect of obstacles and buoyant flow on capture efficiencies of both the traditional flanged and Aaberg hoods. These effects were evaluated based on velocity decay and capture efficiency. Concerning the traditional flanged hood, the obstacle presence had no effect as it was the case with the Aaberg hood. The obstacle caused the flow pattern in front of the hood become deformed and unstable, leading to a deteriorated capture efficiency as the jet entrained the pollution away. Due to Coanda effect, the jet was attracted to the obstacle when it was too close or the obstacle size becomes comparable with the bench-hood distance. When the pollution was generated by a welding process, the flow pattern was influenced by a strong convective plume. The plume influenced performance of both investigated types of hoods in such a way it prevented the pollution generated at the bench from being captured, especially when the hoods were misaligned with the bench surface normal. However, the Aaberg hood compares favourably with the traditional flanged hood when the hood declination is greater than 15°. The poorer performance at low declinations is caused by jet instability. The real performance of the hoods would be even worse because the simulations did not count for crossflow. Unfortunately, the capture efficiency is not the only parameter one has to bear in mind when searching into the local exhaust ventilation. Energy consumption is at the same level of importance. By simple comparison of flow rates, one could conclude the Aaberg hood is superior to the traditional flanged hood as it required less than a half of the air flow rate to achieve its task. But an issue of pressure drop would abate its supremacy over the traditional flanged hood. Investigation of energy consumption, thus, has to follow this research.

## **Acknowledgement**

The research was conducted under financial support of KJB201730501 fund of Grant Agency of the Academy of Sciences of the Czech Republic.

## **References**

- [1] “Newly notified occupational diseases 2004”, Institute of Health Information and Statistics of the Czech Republic, 30 December 2004, [http://www.uzis.cz/cz/archiv05/24\\_05.pdf](http://www.uzis.cz/cz/archiv05/24_05.pdf), (in Czech)
- [2] “Vocational Diseases 2002”, Institute of Health Information and Statistics of the Czech Republic, 30 December 2005, [http://www.uzis.cz/cz/publikac/roc2003\\_cz/nempov2002/np02\\_start.htm](http://www.uzis.cz/cz/publikac/roc2003_cz/nempov2002/np02_start.htm), (in Czech)
- [3] “Unfallstatistik der Arbeitnehmer in der Schweiz: Ergebnisse der fünfjährigen Beobachtungsperiode der SUVA und der UVG-Versicherer”, Technical Report Vol. 15 Periode 15, 1988-92, SUVA, Schweizerische Unfallversicherungsanstalt, SNAIF Swiss National Accident Insurance Fund, Switzerland, 1994
- [4] Aaberg C.P., Plant for Ventilation of Rooms, More Particularly in Stables, United States Patent & Trademark Office, US patent 3401621, 1968
- [5] Hogsted P., Air movements controlled by means of exhaustion, ROOMVENT 1987, International Conference on Air Distribution in Ventilated Spaces, Stockholm, Sweden, 1987
- [6] Hyldgard C.E., Aerodynamic control of exhaust, International Conference on Air Distribution in Ventilated Spaces ROOMVENT 1987, Stockholm, Sweden, 1987
- [7] Pedersen L.G., Reinforced Exhaust System, PhD thesis, Danish Technological Institute, Aarhus, Denmark, 1991
- [8] van Leer B., Towards the ultimate conservative differencing scheme V: A second-order sequel to Godunov's method, J. Comp. Phys., 23, pp. 101136, 1977
- [9] Wilcox D.C., Turbulence Modeling for CFD, DWC Industries inc., La Canada, 2nd edition, USA, 1998
- [10] Krejci V., Kosner J., Flow Pattern generated by a Radial Jet, Proceedings of 8th International Conference VENT 2006, Chicago, USA, 2006
- [11] Havalda, A., Tepelná technika pri zvaraní elektrickým oblúkom (Thermal kinetics of an electric arc welding process), SVTL/SNTL, Bratislava, Slovakia, 1960, (in Slovak)